Bioorganic Chemistry 109 (2021) 104687

Contents lists available at ScienceDirect

Bioorganic Chemistry

journal homepage: www.elsevier.com/locate/bioorg

Synthesis, *in vitro* and computational studies of novel glycosyl-1, 2, 3-1*H*-triazolyl methyl benzamide derivatives as potential α-glucosidase inhibitory activity

Akhilesh Kumar Shukla [a], Manoj Kumar Shrivash [b,c], Anwesh Pandey [c], Jyoti Pandey [a,*]

[a] Department of Chemistry, Babasaheb Bhimrao Ambedkar University, Lucknow, Uttar Pradesh 226025, India
[b] Department of Applied Sciences, Indian Institute Information Technology Allahabad, India
[c] Special Centre for Molecular Medicine, JNU, New Delhi 110067, India

ARTICLE INFO

Keywords:
Benzamide
Click reaction
α-Glucosidase activity
Type-2 diabetes
In-silico-study

ABSTRACT

A series of novel glycosyl-1,2,3-1*H*-triazolyl methyl benzamide analogues were synthesized by the unambiguous strategy and evaluated for α-glucosidase inhibitory activity. Glycosyl benzamide exhibited a dose-dependent inhibition of *α*-glucosidase activity. The *In-vitro* α-glucosidase inhibition activity results indicated that all the synthesized triazolyl methyl benzamide compounds (IC_{50} values ranging from **25.3 ± 0.8** to **118.5 ± 5.3 μM**) exhibited more inhibitory activity in comparison with the standard drug acarbose (IC_{50} = **750.0 ± 12.5 μM**). Among all, the 3 deacetylated glycosyl methyl benzamide derivatives (**4c, 4d** and **4f)** showed promising α-glucosidase enzyme inhibitory activities with IC_{50} value **25.3 ± 0.8, 26.1 ± 1.5 and 30.6 ± 2.1** respectively. Furthermore, these compounds were subjected to molecular docking and molecular dynamics simulation studies. The molecular docking studies were performed between (PDB ID: 3A4A) target protein and these synthesized molecules. The compounds displayed good docking energies in the range of −7.5 to −7.8 Kcal/mol. This work could be used as an initial approach in identifying potential novel molecules with the promising activity of type-2 diabetes mellitus.

1. Introduction

Diabetes mellitus (DM) is a chronic disease of global commons, which tends to have problems with adherence [1,2]. Adherence with medication, diet, and exercise, and blood glucose self–monitoring is quite challenging [3]. Due to consumption of carbohydrate-enriched diet, a metabolic and heterogeneous disorder causing high blood-glucose level, leading to hyperglycaemia [4]. As per the Global Report on Diabetes (2018) by the World Health Organization, diabetes was the seventh major cause of death in 2016[5,6]. Carbohydrates form the largest group of naturally occurring compounds in nature and also crucial due to their pivotal role in medicinal chemistry and drug discovery[7–9]. They are also known for their essential function in development, recognition, growth, function and survival of living cells and organisms. Many drug molecules including several antibiotics and few anti-diabetic medicines contain terminal sugar moieties which are necessary for their biological action [10]. Sugar molecules are benefitted with immense structural diversity which makes it appropriate for library generation of small heterocycles in search of lead molecules[11,12].

They can introduce multiple functionalities in restricted steps. According to estimation, there are more than 194 million people are suffering from diabetes globally that this will increase to 333 million by 2025 [5]. α-Glucosidase is a membrane-bound enzyme that catalyzes the hydrolysis of the glycosidic bond at the non-reducing terminal of the sugar, resulting in the release of free glucose into the digestive tract. They are responsible for glucose absorption and increase glucose concentration in blood. Inhibition of α-glucosidase could diminish the rate of carbohydrates assimilation and concealment of postprandial hyperglycaemia [13]. Along these, α-glucosidase has been regarded as the significant objective for the discovery and development of novel anti-diabetic drugs. As of now, there are three α-glucosidase inhibitors like acarbose, voglibose, and miglitol, which have been utilized in clinical for the treatment of type-2 diabetes mellitus[14,15]. It is proven in literature regularly that the presence of sugar functionality in drug-like molecules alter the bioavailability and efficacy of molecules drastically (Fig. 1). Hence Medicinal Chemists have a tremendous burden of

* Corresponding author.
E-mail address: jyotipandey@bbau.ac.in (J. Pandey).

https://doi.org/10.1016/j.bioorg.2021.104687
Received 14 November 2020; Received in revised form 22 December 2020; Accepted 21 January 2021
Available online 2 February 2021

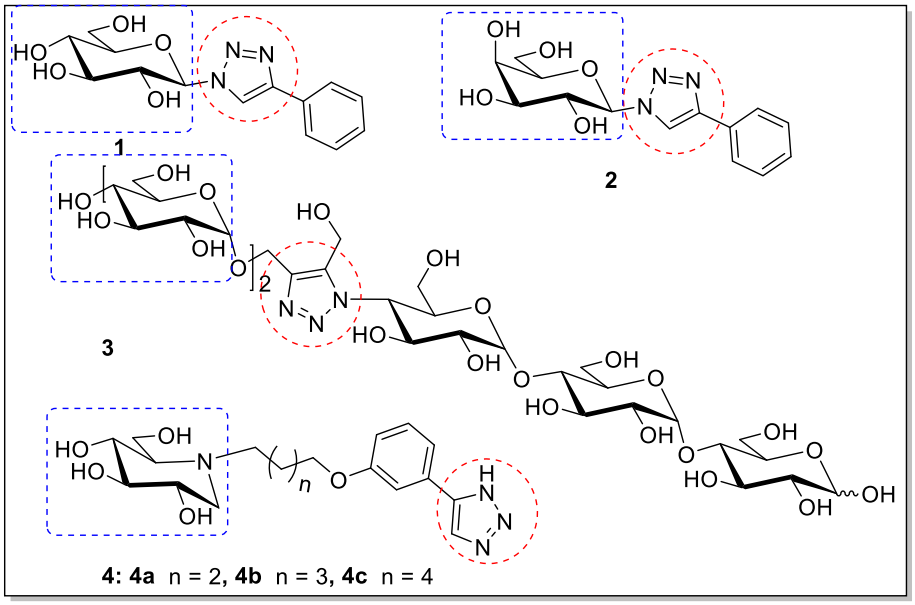

Fig. 1. Potential glycosidase inhibitors synthesised using 'click chemistry': glucosidase 1, galactoside 2, acarbose mimic 3 and MetAP2 II inhibitors 4.

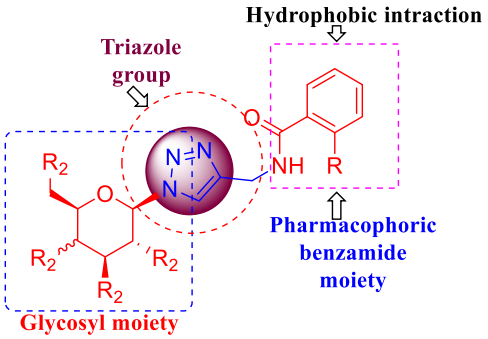

Fig. 2. Designing structure for novel glycosyl benzamides.

developing new molecules with anti-diabetic potential. We hypothesize to couple terminal sugar moiety with aglycon pharmacophore to get better pharmacological property.

Benzamide moiety is very significant class of nitrogen heterocycles and is considered as privileged structure in drug discovery owing to their important roles as key building blocks in the synthesis of many drugs [16]. This heterocyclic nucleus is linked with diverse range of pharmacological activities such as antihypertensive[17], antibacterial[18], anti-inflammatory[19], anticancer[20], analgesic[21],antihistamine [22], CNS stimulant[23] and antidiabetic activities[24].Hence we tried to couple the benzamide nucleus with terminal sugar moieties by applying a suitable and biologically significant linker. 1,2,3-Triazoles are also an essential scaffold in drug discovery and development as several molecules with this moiety exhibited important biological activities such as antifungal[25],antitubercular[26,27] anticancer[28], anti-HIV[29,30] antibacterial[25] antiviral[31] anti-alzheimer[32]anti-mycobacterial[33]and glycosidase inhibitors[34–36]

Keeping the above facts on priority we were prompted to synthesize a novel series of glycohybrids triazoles, consisting of benzamides, triazole and sugars and their inhibition potential was studied against α-glucosidase enzyme in a quest for new anti-diabetic agents (Fig. 2).

2. Results and discussion

2.1. Chemistry

2.1.1. Synthesis of 2-amino-benzamide-4(1H)-ones

2-Amino-*N*-propargyl benzamides (**2a** and **2b**) were prepared from commercially available anthranilic acid (**1a**) and 2-hydroxy-benzoic acid (**1b**) following earlier reported protocols[37] as shown in Scheme 1. The structures were established based on their spectroscopic data [38]. The flask was degassed and then filled with N_2 (balloon), and HOBt (1 mmol), 4- dimethyl aminopyridine (DMAP, 1 mmol) were added to the reaction mixture. Then N, N'-Diisopropylcarbodiimide (DIPC, 1 mmol) was added to the reaction mixture in a dropwise manner. After 10 mins, propargyl amine (1.1 mmol) was added and the reaction was stirred overnight at ambient temperature to get the desired 2-amino-N-(prop-2-yn-1-yl) benzamide (**2a**) 2-hydroxy-N-(prop-2-yn-1-yl) benzamide (**2b**) in 89% yield (Scheme 1).

The structure of the product **2a** was established by their spectroscopic data. ESIMS of the compound displays $m/z = 175$ as $[M + H]^+$ peak corresponding to its molecular formulae $C_{10}H_{11}N_2O$. In IR spectrum, characteristic absorption peaks observed at 3372 cm^{-1} for amine, 3019 cm^{-1} for –NH, 1648 cm^{-1} for carbonyl (–NHC = O). In the ^1H NMR

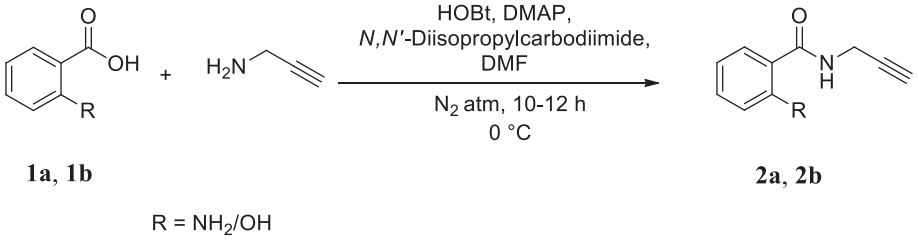

1a, 1b **2a, 2b**

R = NH_2/OH

Scheme 1. Synthesis of 2-amino-*N*-propargyl benzamide derivatives.

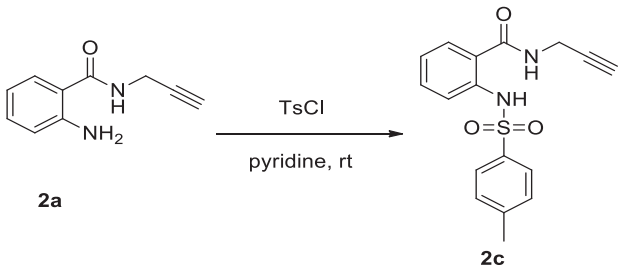

Scheme 2. Synthesis of 2-(4-methylphenylsulfonamido)-N-(prop-2-yn-1-yl) benzamide derivative.

spectrum, the two exchangeable NH_2 protons were observed at δ 5.43 (bs, 2H, –NH_2) and the amide –NH proton was visible at δ 6.25 (bs, 1H, –NH) while the alkynyl proton was visible at δ 2.16 besides other usual protons at their usual chemical shift. In ^{13}C NMR spectrum, the peaks at δ 168.8 accounted for the amide group carbon (–NH-CO-) along with other usual signals. Similarly, the reaction of 2-hydroxy-benzoic acid (**1b**) with propargyl amine the above reaction conditions led to the formation of 2-hydroxy-N-(prop-2-yn-1-yl) benzamide (**2b**) in 88% yield (Scheme 1).

2.1.2. Synthesis of 2-(4-methylphenylsulfonamido)-N-(prop-2-yn-1-yl) benzamide (2c)

2-(4-methylphenylsulfonamido)-*N*-(prop-2-yn-1-yl) benzamide (**2c**) were prepared by following earlier reported protocols[39] as shown in Scheme 2. To a solution of the 2-amino-N-(prop-2-yn-1-yl) benzamide (**2a**, 1.0 equiv) in pyridine (1 M) at room temperature, *p*-toluenesulfonyl chloride (1.05 equiv) was added. The reaction mixture was allowed to stir at room temperature overnight. The reaction mixture was quenched with water, and the aqueous layer was extracted with dichloromethane. The combined organic extracts were washed with aqueous copper sulphate. The organic layer was then dried over magnesium sulphate, filtered, and concentrated under reduced pressure. The residue was purified by column chromatography to afford the desired 2-(4-methylphenylsulfonamido)-*N*-(prop-2-yn-1-yl) benzamide (**2c**) in 79% yield (Scheme 2).

2.1.3. Synthesis of glycosyl triazolyl benzamide-4(3H)-ones

The glycosyl azides(**I** and **II**) were prepared from commercially available glucose and galactose following the methods already reported [40] in the literature as shown in Scheme 3. The structures were established based on their spectroscopic data. These were identical in all respects to those reported earlier[41,42].

The strategy for the synthesis of glycosyl-triazolyl benzamide-4(3*H*)-ones is depicted in Scheme 4. Having the 2-phenyl-3-propargyl-benzamide-4(1*H*)-ones (**2-c**) and glycosyl azides (**I** and **II**) in our hand the CuAAC reactions were performed in *t*-BuOH/H_2O (1:1) using equimolar quantities of the reagents, $CuSO_4{\cdot}5H_2O$ (10 mol%) and sodium ascorbate (20 mol%) at ambient temperature to afford epimeric mixtures of peracetylglycosyl-triazolylbenzamide-4(1*H*)-ones (**3a-f**) in good yields (Scheme 4, Table 1). Propargyl benzamides and glycosyl azides selectively gave only one regioisomer, 1,4-disubstituted triazole via 1,3-dipolar cycloaddition reaction.

The Zemplen deacetylation of the above peracetylated glycosyl triazolyl quinazoline-4(3*H*)-ones (**3a-f**) with NaOMe/MeOH at room temperature led to the formation of the deacetylated glycosyl triazolyl quinazoline-4(3*H*)-ones (**4a-f**) respectively in good yields (Scheme 4, Table 2).

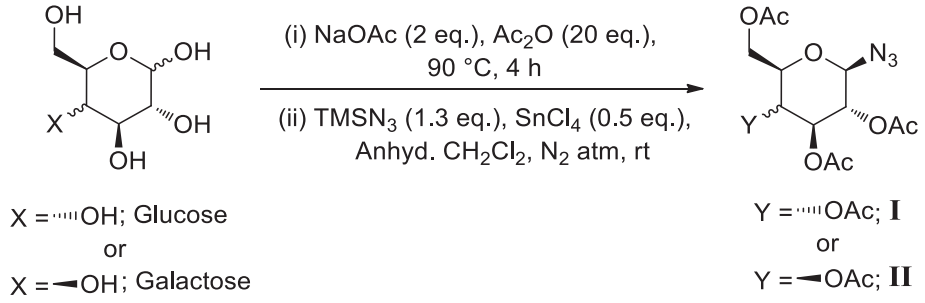

Scheme 3. Synthesis of the glycosyl azides.

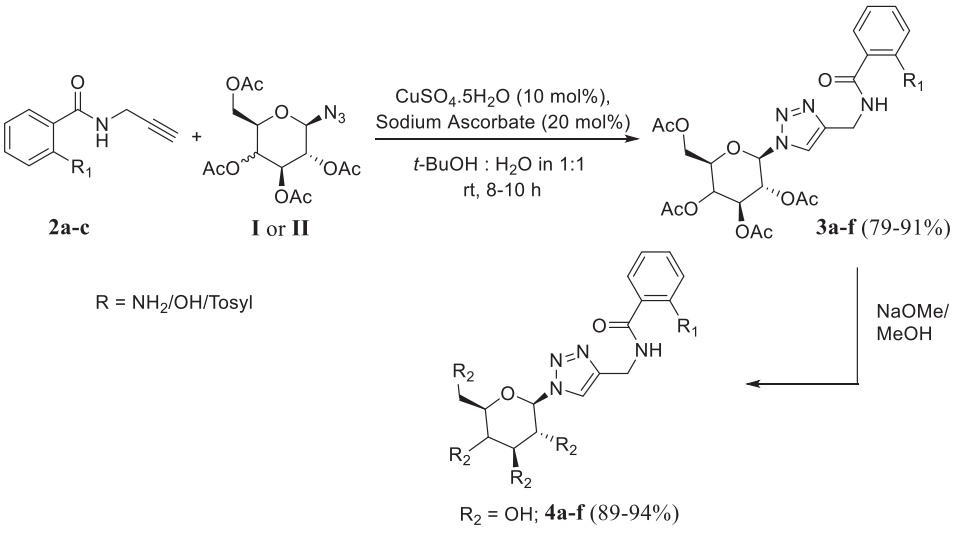

Scheme 4. Synthesis of glycosyl benzamide-4(3*H*)-ones.

Table 1
Peracetylatedglycosyltriazolyl 2-amino-benzamide-4(3*H*)-ones (**4a-f**) from glycosyl azides and 2-amino-benzamide-4(1*H*)-ones.

Entry	2-amino-benzamide-4(1*H*)-ones	Glycosyl Azide	Peracetylatedglycosylbenzamide-4(3*H*)-one	Yield (%)[a]
1	**2a**	**I**	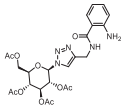 **3a**	80
2	**2a**	**II**	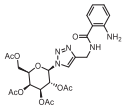 **3b**	78
3	**2b**	**I**	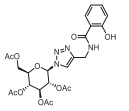 **3c**	77
4	**2b**	**II**	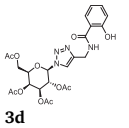 **3d**	75
5	**2c**	**I**	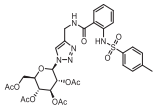 **3e**	73
6	**2c**	**II**	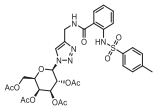 **3f**	71

[a] *Isolated yield as a pure product.*

Table 2
Synthesized deacetylated compounds **4a-f** from per acetylated glycosyl triazolyl quinazoline-4(3*H*)-ones (**3a-f**).

Entry	Peracetylated substrates	Deacetylated products	Yield (%)[a]
1	**3a**	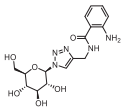 **4a**	94
2	**3b**	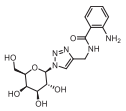 **4b**	92
3	**3c**	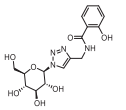 **4c**	93
4	**3d**	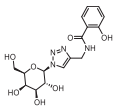 **4d**	91
5	**3e**	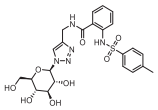 **4e**	92
6	**3f**	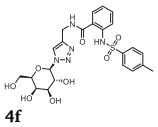 **4f**	90

[a] *Isolated yield as the pure product.*

3. Experimental section

Commercially available reagent grade synthetic compounds were utilized as received. Every reaction was monitored by TLC on E. Merck Kieselgel 60 F254, with detection by UV light, spraying 20% aq $KMnO_4$ solution as well as spraying with 4% ethanolic H_2SO_4. Column chromatography was performed on Silica Gel (60–120 mesh, E. Merck). IR spectra were recorded as thin films or in KBr solution with a Perkin–Elmer Spectrum RX-1 (4000–450 cm^{-1}) spectrophotometer. ^1H and ^{13}C NMR spectra were recorded on Bruker DRX 400 MHz, and 100 MHz instruments, respectively, in $CDCl_3$ and DMSO-d_6. The chemical shift values are reported in ppm concerning TMS (tetramethylsilane) as the internal reference, unless otherwise generally expressed; s (singlet), d (doublet), t (triplet), dd (double doublet), m (multiplet); J in Hertz. ESI mass spectra were performed utilizing a Quattro II (Micromass) instrument. Optical rotations were estimated in a 1.0-dm tube with a Rudolf Autopol III and Horiba polarimeters in $CHCl_3$ and MeOH.

3.1. General procedure for the compounds 2a-b

Anthranilic acid/2-hydroxybenzoic acid (**1a, 1b**, 1 mmol) was added to a 100 mL round bottom flask in dry N, *N*-dimethylformamide (20 mL) equipped with ice. The flask was degassed, then filled with N_2 (balloon), and HOBt (1 mmol), 4- dimethyl aminopyridine (DMAP, 1 mmol) added to the reaction mixture. Then N, N'-Diisopropylcarbodiimide (DIPC, 1 mmol) was added to the solution in dropwise. After 10 mins, propargyl amine (1.1 mmol) was added to the reaction mixture and stirred overnight at ambient temperature. The crude mixture was taken up in water (50 mL) and extracted with ethyl acetate (3 × 40 mL). The combined organic extracts were washed with brine (50 mL), dried over sodium sulphate, filtered, concentrated, and purified by column chromatography (1:1 EtOAc: Hexanes) to afford desired compounds **2a-b**.

3.2. 2-amino-N-(prop-2-yn-1-yl) benzamide (2a)

It was obtained by the reaction of anthranilic acid **1a** (5.0 g, 36.49 mmol) with HOBt (4.92 g, 36.49 mmol), DMAP (4.45 g, 36.49 mmol), DIPC (5.67 mL, 36.49 mmol) and propargyl amine (2.56 mL, 40.14 mmol) in dry DMF (20 mL) in 89% yield (5.65 g) as a white solid; mp 87 °C; IR (ν_{max}, cm^{-1}): 3372, 3019, 1648, 1586, 1403, 1215 and 757.^1H NMR (400 MHz, $CDCl_3$ + CCl_4): δ 7.24 (m, 1H, Ar-H), 7.12 (m, 1H, Ar-H), 6.57 (m, 2H, Ar-H), 6.25 (bs, 1H, –NH), 5.43 (bs, 2H, $–NH_2$), 4.10 (m, 2H, $–CH_2$), 2.16 (m, 1H, –CH). ^{13}C NMR (100 MHz, $CDCl_3$ + CCl_4): δ 168.8 (C═O), 148.9 (Ar-C), 132.6 (Ar-C), 127.2 (Ar-C), 117.3 (Ar-C), 116.5 (Ar-C), 114.9 (Ar-C), 79.7, 71.7 (–CH), 29.4 ($–CH_2$). M.F: $C_{10}H_{11}N_2O$ $[M + H]^+$; ESIMS: *m/z* 175.

3.3. 2-hydroxy-N-(prop-2-yn-1-yl) benzamide (2b)

It was obtained by the reaction of salicylic acid **1b** (5.0 g, 34.70 mmol) with HOBt (4.88 g, 34.70 mmol), DMAP (4.41 g, 34.70 mmol), DIPC (5.32 mL, 34.70 mmol) and propargyl amine (2.46 mL, 34.12 mmol) in dry DMF (20 mL) in 88% yield (5.42 g) as a white solid; mp 86–88 °C; IR (ν_{max}, cm^{-1}): 3372, 3019, 1648, 1586, 1403, 1215 and 757.^1H NMR (400 MHz, $CDCl_3$ + CCl_4): δ 7.24 (m, 1H, Ar-H), 7.12 (m, 1H, Ar-H), 6.57 (m, 2H, Ar-H), 6.25 (bs, 1H, –NH), 5.43 (bs, 2H, $–NH_2$), 4.10 (m, 2H, $–CH_2$), 2.16 (m, 1H, –CH). ^{13}C NMR (100 MHz, $CDCl_3$ + CCl_4): δ 168.8 (C═O), 148.9 (Ar-C), 132.6 (Ar-C), 127.2 (Ar-C), 117.3 (Ar-C), 116.5 (Ar-C), 114.9 (Ar-C), 79.7, 71.7 (–CH), 29.4 ($–CH_2$). M.F:

$C_{10}H_9NO_2$ $[M + H]^+$; ESIMS: *m/z* 175.

3.4. 2-(4-methylphenylsulfonamido)-N-(prop-2-yn-1-yl)benzamide (2c)

It was obtained by the reaction the 2-amino-N-(prop-2-yn-1-yl) benzamide (**2a**, 2.0 g, 13.28 mmol) in pyridine (5 mL) at room temperature with *p*-toluenesulfonyl chloride (5.05 mL) wad added. The reaction mixture was allowed to stir at room temperature overnight and extracted with DCM to give the crude product, which was purified by column chromatography (20% EtOAc/Hexane) to give the title compound (**2c**) in79% yield (g) as a white solid; mp 87 °C; IR (ν_{max}, cm^{-1}): 3376, 3028, 1644, 1307, 1215, 1173, 907 and 669.^{1}H NMR (400 MHz, $CDCl_3 + CCl_4$): δ7.76 (bs, 1H, –NH), 7.54 (m, 2H, Ar-H), 7.32 (m, 2H, Ar-H), 7.12 (m, 2H, Ar-H), 6.94(m, 2H, Ar-H), 4.10 (m, 2H, $–CH_2$), 2.36 (m, 3H, $–CH_3$), 2.16 (m, 1H, –CH). ^{13}C NMR (100 MHz, $CDCl_3 + CCl_4$): δ 169.3 (C═O), 149.7 (Ar-C), 132.8 (Ar-C), 127.2 (2C, Ar-C), 118.3 (2C, Ar-C), 117.5 (Ar-C), 115.9 (Ar-C), 79.7, 71.7 (–CH), 29.3 ($–CH_2$), 21.6 ($–CH_3$);M.F: $C_{17}H_{16}N_2O_3S$ $[M + H]^+$; ESIMS: *m/z* 329.09.

3.5. 2-amino-N-[(1-(1′-deoxy-2′, 3′, 4′, 6′-tetra-O-acetyl-β-D-glucopyranos-1′-yl)]-1H-1, 2, 3-triazol-4-yl) methyl-benzamide (3a)

It was obtained by the reaction of **2a** (0.50 g, 1.89 mmol), azido sugar **I** (0.72 g, 1.89 mmol), $CuSO_4{\cdot}5H_2O$ (0.042 g, 0.16 mmol) and sodium ascorbate (0.071 g, 0.35 mmol) in 1:1 *tert*-Butanol-water (40 mL) in 80% yield (1.03 g) as a white solid; mp 106–108 °C; IR (ν_{max}, cm^{-1}): 3290, 2349, 1607, 1523, 1245, 1217, 1182, 758 and 669.^{1}H NMR (400 MHz, $CDCl_3 + CCl_4$): δ 7.83 (s, 1H, triazolyl-H), 7.35 (m, 1H, Ar-H), 7.26 (m, 1H, Ar-H), 6.81 (bs, 1H, –NH), 6.66 (m, 2H, Ar-H), 5.82 (d, $J = 9.2$ Hz, 1H, H-1́), 5.52–5.47 (m, 2H, H-2́, H-3́), 5.25 (m, 1H, H-4́), 4.74 (m, 2H, $–CH_2$), 4.24–4.09 (m, 2H, H-5́, H-6′), 2.22 (s, 3H, $–OCOCH_3$), 2.03 (s, 3H, $–OCOCH_3$), 2.00 (s, 3H, $–OCOCH_3$), 1.87 (s, 3H, $–OCOCH_3$).^{13}C NMR (100 MHz, DMSO-d_6): δ 170.4, 170.3, 169.9, 168.9, 150.2, 146.3, 132.3, 128.6, 122.7, 116.8, 115.0, 114.6, 84.6, 73.4, 70.9, 68.0, 67.8, 62.0, 34.8, 20.9, 20.8, 20.7, 20.4; HRMS: Calcd. Accurate mass for ($C_{24}H_{29}N_5O_{10}$): 548.1914. Found 548.1956 $[M + H]^+$.

3.6. 2-amino-N-[(1-(1′-deoxy-2′, 3′, 4′, 6′-tetra-O-acetyl-β-D-galactopyranose-1′-yl)]-1H-1, 2, 3-triazol-4-yl) methyl)-benzamide (3b)

It was obtained by the reaction of **2a** (0.50 g, 1.89 mmol), azido sugar **II** (0.72 g, 1.89 mmol), $CuSO_4{\cdot}5H_2O$ (0.042 g, 0.16 mmol) and sodium ascorbate (0.071 g, 0.35 mmol) in 1:1 *tert*-Butanol-water (40 mL) in 78% yield (1.08 g) as a yellow solid; mp 118–120 °C; IR (ν_{max}, cm^{-1}): 3292, 2365, 1610, 1535, 1230, 1216, 1184, 771 and 669.^{1}H NMR (400 MHz, $CDCl_3 + CCl_4$): δ 7.88 (s, 1H, triazolyl-H), 7.37 (m, 1H, Ar-H), 7.20 (m, 1H, Ar-H), 6.91 (bs, 1H, –NH), 6.66 (m, 2H, Ar-H), 5.82 (d, $J = 9.2$ Hz, 1H, H-1́), 5.52–5.47 (m, 2H, H-2́, H-3́), 5.25 (m, 1H, H-4́), 4.74 (m, 2H, $–CH_2$), 4.24–4.09 (m, 2H, H-5́, H-6′), 2.22 (s, 3H, $–OCOCH_3$), 2.03 (s, 3H, $–OCOCH_3$), 2.00 (s, 3H, $–OCOCH_3$), 1.87 (s, 3H, $–OCOCH_3$).^{13}C NMR (100 MHz, DMSO-d_6): δ 170.4, 170.3, 169.9, 168.9, 150.2, 146.3, 132.3, 128.6, 122.7, 116.8, 115.0, 114.6, 84.6, 73.4, 70.9, 68.0, 67.8, 62.0, 34.8, 20.9, 20.8, 20.7, 20.4; HRMS: Calcd. Accurate mass for ($C_{24}H_{29}N_5O_{10}$): 548.1914. Found 548.1952 $[M + H]^+$.

3.7. 2-hydroxy-N-[(1-(1′-deoxy-2′, 3′, 4′, 6′-tetra-O-acetyl-β-D-glucopyranos-1′-yl)]-1H-1,2,3-triazol-4′-yl)methyl-benzamide (3c)

It was obtained by the reaction of **2b** (0.53 g, 1.85 mmol), azido sugar **I** (0.73 g, 1.89 mmol), $CuSO_4{\cdot}5H_2O$ (0.042 g, 0.16 mmol) and sodium ascorbate (0.071 g, 0.35 mmol) in 1:1 *tert*-Butanol-water (40 mL) in 77% yield (1.06 g) as a white solid; mp 111–113 °C; IR (ν_{max}, cm^{-1}): 3449, 2395, 1620, 1534, 1230, 1218, 1185 and 754.^{1}H NMR (400 MHz, DMSO-d_6): δ 12.40 (m, 1H, –NH), 9.22 (s, 1H, triazolyl-H), 7.37 (m, 1H, Ar-H), 7.20 (m, 1H, Ar-H), 6.66 (m, 2H, Ar-H),6.20 (m, 1H, –OH), 5.82 (d, $J = 9.2$ Hz, 1H, H-1́), 5.52–5.47 (m, 2H, H-2́, H-3́), 5.25 (m, 1H, H-4́), 4.74 (m, 2H, $–CH_2$), 4.24–4.09 (m, 2H, H-5́, H-6′), 2.22 (s, 3H, $–OCOCH_3$), 2.03 (s, 3H, $–OCOCH_3$), 2.00 (s, 3H, $–OCOCH_3$), 1.87 (s, 3H, $–OCOCH_3$).^{13}C NMR (100 MHz, DMSO-d_6): δ 170.0, 169.5, 169.2, 168.4(4 × $–COCH_3$), 160.8(–CO), 145.4(Ar-C), 133.8(Ar-C), 128.0(Ar-C), 122.4(Ar-C), 118.6(Ar-C), 117.6(Ar-C), 115.2(Ar-C), 96.0 (C-1′), 84.4(C-5′), 79.0(C-3′), 78.6(C-4′), 73.9(C-2′), 72.8(C-6′), 70.5, 67.9, 61.9, 40.3($–CH_2$), 39.8, 34.8,20.8, 20.6, 20.5, 20.2(4 × $–OCOCH_3$); HRMS: Calcd. Accurate mass for ($C_{24}H_{28}N_4O_{11}$): 549.1755. Found 549.1792 $[M + H]^+$.

3.8. 2-hydroxy-N-[(1-(1′-deoxy-2′,3′,4′,6′-tetra-O-acetyl-β-D-galactopyranose-1′-yl)]-1H-1, 2, 3-triazol-4-yl)methyl-benzamide (3d)

It was obtained by the reaction of **2b** (0.53 g, 1.85 mmol), azido sugar **II** (0.73 g, 1.89 mmol), $CuSO_4{\cdot}5H_2O$ (0.042 g, 0.16 mmol) and sodium ascorbate (0.071 g, 0.35 mmol) in 1:1 *tert*-Butanol-water (40 mL) in 75% yield (1.07 g) as a yellow solid; mp 120–122 °C; IR (ν_{max}, cm^{-1}): 3434, 2381, 1625, 1537, 1226, 1217, 1184, 753 and 659.^{1}H NMR (400 MHz, $CDCl_3$): δ 12.18(m, 1H, –NH), 7.90 (s, 1H, triazolyl-H), 7.53 (m, 1H, Ar-H), 7.47 (m, 1H, Ar-H), 7.37 (m, 2H, Ar-H),6.82 (m, 1H, –OH), 5.83(d, $J = 9.2$ Hz, 1H, H-1́), 5.52–5.47 (m, 2H, H-2́, H-3́), 5.26 (m, 1H, H-4́), 4.78 (m, 2H, $–CH_2$), 4.24–4.09 (m, 2H, H-5́, H-6′), 2.22 (s, 3H, $–OCOCH_3$), 2.03 (s, 3H, $–OCOCH_3$), 2.00 (s, 3H, $–OCOCH_3$), 1.87 (s, 3H, $–OCOCH_3$).^{13}C NMR (100 MHz, $CDCl_3$): δ 169.9, 169.7, 168.4, 168.7(4 × $–COCH_3$), 161.7(–CO), 144.8(Ar-C), 134.1(Ar-C), 125.8(Ar-C), 121.3(Ar-C), 118.5(Ar-C), 114.0(Ar-C), 86.3(C-1′), 77.2(C-5′), 76.9 (C-3′), 74.0(C-4′), 70.6(C-2′), 68.0(C-6′), 34.6($–CH_2$), 20.5, 20.5, 20.4, 20.1(4 × $–OCOCH_3$); HRMS: Calcd. Accurate mass for ($C_{24}H_{28}N_4O_{11}$): 549.1755 Found 549.1796 $[M + H]^+$.

3.9. 4-methyl-N-[(1-(1′-deoxy-β-D-glucopyranos-1′-yl)]-1H-1,2,3-triazol-4-yl)methyl-benzenesulphonamide (3e)

It was obtained by the reaction of **2c** (0.1 g, 0.66 mmol), azido sugar **I** (0.25 g, 0.66 mmol), $CuSO_4{\cdot}5H_2O$ (0.02 g, 0.06 mmol) and sodium ascorbate (0.03 g, 0.13 mmol) in 1:1 *tert*-butanol-water (20 mL) in 73% yield (0.32 g) as a white solid; m.p. 86–88 °C;IR (ν_{max}, cm^{-1}): 3245, 2371, 1658, 1510, 1309, 1227, 1169 and 768.^{1}H NMR (400 MHz, DMSO-d_6): δ 10.74 (s, 1H, –NH), 7.91 (s, 1H, triazolyl-H), 7.61 (m, 3H, Ar-H), 7.40 (m, 2H, Ar-H), 7.26 (m, 2H, Ar-H), 7.11 (m, 2H, Ar-H), 6.98 (m, 2H, Ar-H), 5.88 (d, $J = 9.1$ Hz, 1H, H-1́),5.48–5.42 (m, 2H, H-2́, H-3́), 5.26 (m, 1H, H-4́), 4.60 (m, 2H, $–CH_2$),4.29–4.12 (m, 2H, H-5́, H-6′),2.32 (s, 3H, $–OCOCH_3$), 2.06(s, 3H, $–OCOCH_3$), 2.03(s, 3H, $–OCOCH_3$), 1.86(s, 3H, $–OCOCH_3$).^{13}C NMR (100 MHz, $CDCl_3$) δ 170.2, 169.7, 169.0, 168.6, 168.3, 143.3, 139.0, 136.6, 132.6, 129.4, 127.2, 127.0, 123.3, 121.0, 120.9, 96.1, 85.8, 77.2, 76.9, 76.6, 75.2, 72.6, 70.4, 67.6, 61.3, 35.1, 21.4, 20.5, 20.4, 20.1. HRMS: Calcd. Accurate mass for ($C_{31}H_{35}N_5O_{12}S$): 702.2003. Found 702.2042 $[M + H]^+$.

3.10. 4-methyl-N-[(1-(1′-deoxy-β-D-galactopyranose-1′-yl)]-1H-1,2,3-triazol-4-yl)methyl-benzenesulphonamide (3f)

It was obtained by the reaction of **2c** (0.1 g, 0.66 mmol), azido sugar **II** (0.25 g, 0.66 mmol), $CuSO_4{\cdot}5H_2O$ (0.02 g, 0.06 mmol) and sodium ascorbate (0.03 g, 0.13 mmol) in 1:1 *tert*-butanol-water (20 mL) in 71% yield (0.30 g) as a white solid; m.p. 86–88 °C;IR (ν_{max}, cm^{-1}): 3242, 2374, 1661, 1512, 1307, 1228, 1163 and 768.^{1}H NMR (400 MHz, DMSO-d_6): δ δ 10.74 (s, 1H, –NH), 7.94 (s, 1H, triazolyl-H), 7.64 (m, 3H, Ar-H), 7.43 (m, 2H, Ar-H), 7.26 (m, 2H, Ar-H), 7.13 (m, 2H, Ar-H), 6.99 (m, 2H, Ar-H), 5.85 (d, $J = 9.1$ Hz, 1H, H-1́),5.57–5.52 (m, 2H, H-2́, H-3́), 5.26 (m, 1H, H-4́), 4.63 (m, 2H, $–CH_2$), 4.25–4.19 (m, 2H, H-5́, H-6′), 2.32 (s, 3H, $–OCOCH_3$), 2.23 (s, 3H, $–OCOCH_3$), 2.01 (s, 3H, $–OCOCH_3$), 1.88 (s, 3H, $–OCOCH_3$).^{13}C NMR (100 MHz, $CDCl_3$) δ 170.0, 169.8, 169.5, 168.8(4 × $–COCH_3$), 168.3(–CO), 144.4 (Ar-C), 143.3 (Ar-C), 139.0 (Ar-C), 136.7 (Ar-C), 132.6 (Ar-C), 129.4 (Ar-C), 127.3 (Ar-C), 127.2 (Ar-C), 127.0, 123.3, 121.4, 121.0, 121.0, 96.1, 86.3, 77.2, 76.9,

76.6, 74.1, 70.7, 68.0, 66.7, 61.0, 42.1, 35.1, 23.5, 21.4, 20.1, 20.5, 20.4, 20.2. HRMS: Calcd. Accurate mass for ($C_{31}H_{35}N_5O_{12}S$): 702.2003. Found 702.2045 $[M + H]^+$.

3.11. 2-amino-N-[(1-(1′-deoxy-β-D-glucopyranos-1′-yl)]-1H-1,2,3-triazol-4-yl)methyl-benzamide (4a)

It was obtained by treating the acetylated compound **3a** (0.40 g, 0.63 mmol) with NaOMe in methanol, in 94% yield (0.27 g) as a white solid;; mp 83–85 °C;$[\alpha]_D^{25}$ 0.4 (c 0.1, CH_3OH); IR (ν_{max}, cm^{-1}): 3411, 3019, 1638, 1215 and 758.^{1}H NMR (400 MHz, DMSO-d_6): δ 8.74 (m, 1H, –NH), 8.08 (s, 1H, triazolyl-H), 7.53 (d, J = 6.9 Hz, 1H, Ar-H), 7.16 (m, 1H, Ar-H,), 6.70 (d, J = 8.0 Hz, 1H, Ar-H), 6.53 (t, J = 7.7 Hz, 1H, Ar-H), 6.41 (bs, 2H, –NH_2), 5.51 (d, J = 9.3 Hz, 1H, H-1́), 5.38 (m, 1H, –OH), 5.26 (m, 1H, –OH), 5.17 (m, 1H, –OH),4.68 (m, 1H, –OH), 4.48 (m, 2H, –CH_2), 3.78–3.59 (m, 4H, H-2′, H-3′, H-4′, H-5′), 3.25 (m, 2H, H-6′).^{13}C NMR (100 MHz, DMSO-d_6): δ 169.3 (C═O), 150.1 (Ar-C), 145.8 (Ar-C), 132.3 (Ar-C), 128.6 (Ar-C), 122.4(Ar-C), 116.8 (Ar-C), 115.1 (Ar-C), 114.5 (Ar-C), 87.8 (C-1́), 80.3 (C-5́), 77.4 (C-3́), 72.4 (C-4́), 69.9 (C-2́), 61.1 (C-6́), 34.8 (–CH_2). HRMS: Calcd. Accurate mass for ($C_{16}H_{21}N_5O_6$): 380.1492. Found 380.1531 $[M + H]^+$.

3.12. 2-amino-N-[(1-(1′-deoxy-β-D-galactopyranose-1′-yl)]-1H-1,2,3-triazol-4-yl)methyl-benzamide(4b)

It was obtained by treating the acetylated compound **3b** (0.40 g, 0.63 mmol) with NaOMe in methanol, in 92% yield (0.26 g) as a white solid; mp 64–66 °C;$[\alpha]_D^{25}$ 1.3 (c 0.1, CH_3OH); IR (ν_{max}, cm^{-1}): 3400, 3019, 1644, 1215 and 769.^{1}H NMR (400 MHz, DMSO-d_6): δ 8.77 (m, 1H, –NH), 8.04 (s, 1H, triazolyl-H), 7.53 (m, 1H, Ar-H), 7.16 (m, 1H, Ar-H), 6.70 (m, 1H, Ar-H), 6.53 (m, 1H, Ar-H), 5.47 (d, J = 9.1 Hz, 1H, H-1́), 4.48 (m, 2H, –CH_2), 4.02 (m, 2H, H-5′, –OH), 3.75 (m, 3H, 3 × –OH), 3.70 (m, 4H, H-2′, H-3′, H-4́, H-6́), 3.17 (bs, 2H, –NH_2).^{13}C NMR (100 MHz, DMSO-d_6): δ 169.3 (C═O), 150.1 (Ar-C), 145.9 (Ar-C), 132.3, 128.6 (Ar-C), 122.0, 116.9 (Ar-C), 115.1 (Ar-C), 114.5 (Ar-C), 88.4 (C-1́), 78.8 (C-5́), 74.1 (C-3́), 69.8 (C-4́), 68.9 (C-2́), 60.8 (C-6′), 34.9. HRMS: Calcd. Accurate mass for ($C_{16}H_{21}N_5O_6$): 380.1492. Found 380.1528 $[M + H]^+$.

3.13. 2-hydroxy-N-[(1-(1′- deoxy-β-D-glucopyranos-1′-yl)]-1H-1,2,3-triazol-4-yl)methyl-benzamide (4c)

It was obtained by treating the acetylated compound **3c** (0.40 g, 0.60 mmol) with NaOMe in methanol in 93% yield (0.27 g) as a white solid; mp 84–86 °C;$[\alpha]_D^{25}$ – 2.4 (c 0.1, CH_3OH); IR (ν_{max}, cm^{-1}): 3670, 3401, 3018, 1644, 1215 and 757.^{1}H NMR (400 MHz, DMSO-d_6): δ 8.74 (m, 1H, –NH), 7.94 (s, 1H, triazolyl-H), 7.53 (m, 1H, Ar-H), 7.15 (m, 1H, Ar-H), 6.72 (m,1H, Ar-H), 6.52 (m, 1H, Ar-H), 6.43 (bs, 1H, –OH), 5.88 (d, J = 9.3 Hz, 1H, H-1́), 5.38 (m, 1H, –OH), 5.26 (m, 1H, –OH), 5.17 (m, 1H, –OH),4.68 (m, 1H, –OH), 4.48 (m, 2H, –CH_2), 3.78–3.59 (m, 3H, H-2′, H-3′, H-4′), 3.25 (m, 2H, H-5′, H-6′)^{13}C NMR (100 MHz, DMSO-d_6): δ 169.2 (C═O), 150.1(Ar-C), 145.8(Ar-C), 132.2(Ar-C), 128.6(Ar-C), 123.8(Ar-C), 116.8(Ar-C), 114.7(Ar-C), 111.2, 104.9, 85.4, 79.6, 74.0, 49.2, 34.9, 27.0, 26.HRMS: Calcd. Accurate mass for ($C_{18}H_{23}N_5O_5$): 390.1699. Found 390.1735 $[M + H]^+$.

3.14. 2-hydroxy-N-[(1-(1′-deoxy-β-D-galactopyranose-1′-yl)]-1H-1,2,3-triazol-4-yl)methyl-benzamide (4d)

It was obtained by treating the acetylated compound **3d** (0.40 g, 0.58 mmol) with NaOMe in methanol in 91% yield (0.26 g) as a yellow solid; mp 73–75 °C;$[\alpha]_D^{25}$ – 1.6 (c 0.1, CH_3OH); IR (ν_{max}, cm^{-1}): 3408, 3019, 1753, 1644, 1215 and 769.^{1}H NMR (400 MHz, DMSO-d_6): δ 12.43 (s, 1H, –NH), 9.35 (s, 1H, triazolyl-H), 8.13 (s, 1H, Ar-H), 7.90 (m, 1H, Ar-H), 7.43 (m, 1H, Ar-H), 7.39 (m, 1H, Ar-H), 6.92 (d, J = 9.1 Hz, 1H, H-1́), 5.48 (m, 2H, –CH_2), 5.21 (m, 1H, –OH), 4.59 (m, 2H, H-5′, –OH), 4.09 (m, 3H, 3 × –OH), 3.75–3.34 (m, 5H, H-2′, H-3′, H-4́, H-6́), ^{13}C NMR (100 MHz, DMSO-d_6): δ 169.2(–CO), 160.3(Ar-C), 144.9(Ar-C), 134.2(Ar-C), 128.4(Ar-C), 122.2(Ar-C), 119.1(Ar-C), 117.8(Ar-C), 115.7 (Ar-C), 88.5(C-1′), 78.8(C-5′), 74.1(C-3′), 69.7(C-4′), 68.9(C-2′), 60.8(C-6′), 40.6(–CH_2);HRMS: Calcd. Accurate mass for ($C_{16}H_{20}N_4O_7$): 381.1332. Found 381.1372 $[M + H]^+$.

Table 3
α-Glucosidase inhibitory activity (10 μM) of the synthesized benzamide analogues.

S.No.	Code	% α-Glucosidase inhibition	IC_{50}(μM)[a]
1.	**3a**	5.18	112.4 ± 6.3
2.	**3b**	6.21	118.5 ± 5.3
3.	**3c**	22.7	104.3 ± 6.0
4.	**3d**	26.9	107.6 ± 7.1
5.	**3e**	15.7	109.7 ± 2.8
6.	**3f**	17.3	113.2 ± 1.0
7.	**4a**	35.7	48.5 ± 1.5
8.	**4b**	36.9	52.6 ± 2.1
9.	**4c**	39.7	**25.3 ± 0.8**
10.	**4d**	40.6	**26.1 ± 1.5**
11.	**4e**	24.6	43.7 ± 1.8
12.	**4f**	42.9	**30.6 ± 2.1**
13.	**Acarbose**	**53.4**	750.0 ± 12.5

[a] Data expressed as the mean of ± S.E. of at least 3 different experiments.

3.15. 4-methyl-N-[(1-(1′-deoxy-β-D-glucopyranos-1′-yl)]-1H-1,2,3-triazol-4-yl)methyl-benzenesulphonamide (4e)

It was obtained by treating the acetylated compound **3e** (0.40 g, 0.59 mmol) with NaOMe in methanol in 92% yield (0.26 g) as a white solid; mp 88–90 °C;$[\alpha]_D^{25}$ – 1.2 (c 0.1, CH_3OH); IR (ν_{max}, cm^{-1}): 3408, 3019, 1753, 1644, 1215 and 769.^{1}H NMR (400 MHz, DMSO-d_6): δ 11.56 (s, 1H, –NH), 9.33 (s, 1H, triazolyl-H), 8.17 (s, 1H, Ar-H), 7.74 (m, 1H, Ar-H), 7.63 (m, 2H, Ar-H), 7.46 (m, 2H, Ar-H), 7.30 (m, 2H, Ar-H),7.11 (d, J = 9.1 Hz, 1H, H-1́), 5.55 (m, 2H, –CH_2), 5.52 (m, 1H, –OH), 4.50 (m, 2H, H-5′, –OH), 3.80 (m, 3H, 3 × –OH), 3.76–3.67 (m, 4H, H-2′, H-3′, H-4́, H-6́),2.31 (s, 3H, –CH_3).^{13}C NMR (100 MHz, DMSO) δ 168.5, 144.6, 144.3, 138.8, 136.0, 133.1, 130.3, 128.9, 127.2, 123.8, 122.7, 119.9, 87.8, 80.3, 77.4, 72.4, 70.0, 40.4, 40.2, 40.0, 39.8, 39.8, 39.5, 39.3, 39.1, 35.1, 21.4. HRMS: Calcd. Accurate mass for ($C_{23}H_{27}N_5O_8S$): 534.1580. Found 534.1621 $[M + H]^+$.

3.16. 4-methyl-N-[(1-(1′-deoxy-β-D-galactopyranose-1′-yl)]-1H-1,2,3-triazol-4-yl)methyl-benzenesulphonamide (4f).

It was obtained by treating the acetylated compound **3f** (0.40 g, 0.59 mmol) with NaOMe in methanol in 90% yield (0.25 g) as a white solid; mp 83–85 °C;$[\alpha]_D^{25}$ – 5.4 (c 0.1, CH_3OH); IR (ν_{max}, cm^{-1}): 3408, 3019, 1753, 1644, 1215 and 769.^{1}H NMR (400 MHz, DMSO-d_6): δ 11.60 (s, 1H, –NH), 9.34 (s, 1H, triazolyl-H), 8.15 (s, 1H, Ar-H), 7.75 (m, 1H, Ar-H), 7.63 (m, 2H, Ar-H), 7.51 (m, 2H, Ar-H), 7.31 (m, 2H, Ar-H), 7.13 (d, J = 9.1 Hz, 1H, H-1́), 5.51 (m, 2H, –CH_2), 4.51 (m, 1H, –OH), 4.08 (m, 2H, H-5′, –OH), 3.78 (m, 3H, 3 × –OH), 3.57–3.45 (m, 4H, H-2′, H-3′, H-4́, H-6́),2.31 (s, 3H, –CH_3).^{13}C NMR (100 MHz, DMSO) δ 168.5, 144.6, 144.3, 138.9, 136.1, 133.1, 130.3, 128.9, 127.2, 123.8, 122.3, 120.6, 120.0, 88.5, 78.8, 74.2, 69.8, 68.8, 60.8, 49.0, 40.5, 40.3, 40.1, 39.9, 39.7, 39.5, 39.3, 35.2, 23.7, 21.4. HRMS: Calcd. Accurate mass for ($C_{23}H_{27}N_5O_8S$): 534.1580. Found 534.1618 $[M + H]^+$.

4. Biology

The compounds synthesized glycosyl 1,2,3-1H-triazolyl methyl benzamide derivatives were evaluated against the α-glucosidase purified from rat intestine, purified rat liver following earlier protocols [43,44]. The *In-vitro* α-glucosidase inhibition activity results indicated that all the synthesized compounds (IC_{50} values ranging from 25.3 ± 0.8 to 118.5 ±

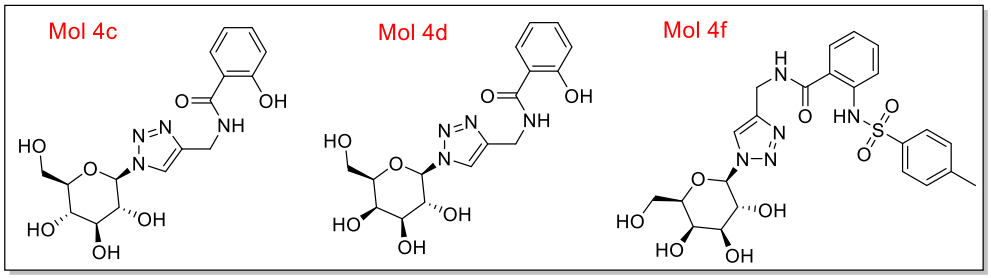

Fig 3. Figure showing chemical structures of the selected active molecules.

5.3 μM) exhibited more inhibitory activity in comparison to standard drug acarbose ($IC_{50} = 750.0 \pm 12.5$ μM). The percent inhibitory activity of screened compounds against *α*-glucosidase enzyme and IC_{50}value of all the compounds have been shown in Table 3 and evidently, most of the triazolo-methyl benzamide derivative with deacetylated sugar unit displayed better *α*-enzyme inhibition than that of analogues with acetylated sugar unit. The deacetylated glycosyl methyl benzamide derivative (**4c, 4d** and **4f)** IC_{50} value **25.3 ± 0.8,26.1 ± 1.5** and **30.6 ± 2.1** respectively.

5. Preparation of α-Glucosidase from rat intestinal mucosa

α-Glucosidase was prepared according to a slight modification of the procedure reported earlier [43,44]. The intestine of male albino rats (CF strain average body weight 200 ± 20 g) was excised opened and the mucosa was collected and pooled. A 10% homogenate was prepared in 150 mM KCl using Potter Elvejhem glass homogeniser fitted with Teflon pestle. The homogenate was centrifuged at 1000*g* for 15 min and the supernatant was decanted and stored at 4 °C. The supernatant was dialyzed at 4 °C against 50 mM Tris–HCl buffer pH 7.0 with two to three changes of buffer. The dialyzed supernatant was saturated with ammonium sulphate to a final concentration of 30%. The sample was kept at 4 °C overnight and then centrifuged to collect the precipitate and the supernatant separately. The 30% ammonium sulphate saturated supernatant was further saturated to 60% with ammonium sulphate. Again the precipitate and supernatant were separated by centrifugation. Finally, the 60% ammonium sulphate saturated supernatant was further saturated to 100% with a further addition of ammonium sulphate. The precipitate and supernatant were once again separated and all the samples were analysed for α-glucosidase activity using *p*-nitrophenyl-α-D-glucopyranoside as substrate. When it was observed that the enzyme activity is maximum in 60–100% ammonium sulphate precipitate it was stored at 4 °C and used as a source of enzyme for studying the effect of test compounds on α-glucosidase inhibition.

6. Computational methodology

6.1. System selection and preparation

The lead molecules (Mol-4c, Mol-4d & Mol-4f) that had good biological activities were selected for computational studies. Their chemical structures are shown in (Fig. 3). The protein, 3A4A [45] was obtained from Protein Data Bank [46]. Water molecules, from selected protein, were removed using UCSF Chimera before the start of docking calculations [47].

6.2. Molecular docking calculations

Molecular Docking is a widely used computational technique that predicts the binding of potent inhibitors in the vicinity of the target macromolecules [48,49]. The ability to determine the binding affinity and main interacting protein residues are the key objectives of molecular docking of protein–ligand complexes [50]. Here, the docking calculation was carried out using Schrödinger's GLIDE module [51]. The docked pose with the least binding affinity was extracted and aligned with the receptor for further analysis.

6.3. Molecular dynamics simulation

MDS is a widely used computational technique to study protein folding, unwinding and other conformational changes including complex stability, over a specified period. Its applications have gained utmost importance due to lack of experimental resources [52]. GROMACS 5.1.1 (Groningen Machine for Chemical Simulations) software package [53] was used to carry out the molecular dynamics simulations in the current research work. A total of two ligand–protein complexes were created, after docking simulations for molecular dynamic simulations viz., (Mol-4c, Mol-4d & Mol-4f) (Fig. 4). These ligand–protein complexes were put to for 10000 ps (10 ns) time scale simulation. There are many studies for the comparison of force fields for the nucleic acids but GROMOS54A7 force fields [54] seems to be good for nucleic acid simulation due to the presence of specific topologies for the terminal nucleotides. The topology for the selected ligands was obtained using PRODRG web server [55]. The protein–ligand complexes were solvated

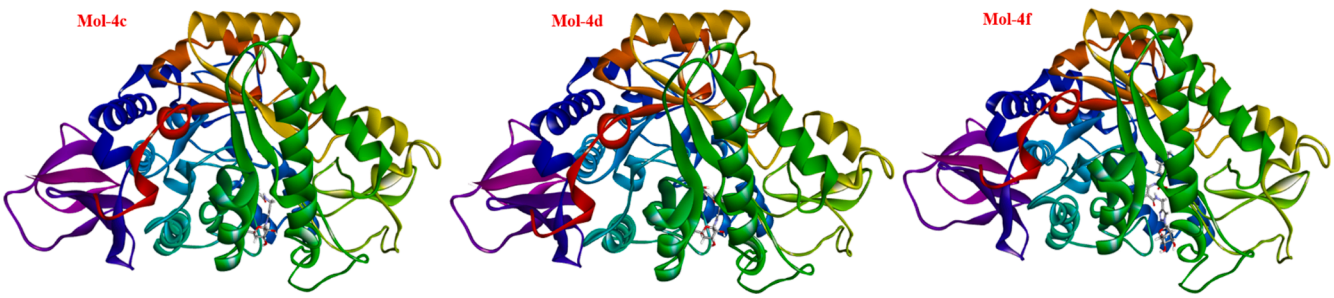

Fig 4. Figure showing best docked posed protein–ligand complexes.

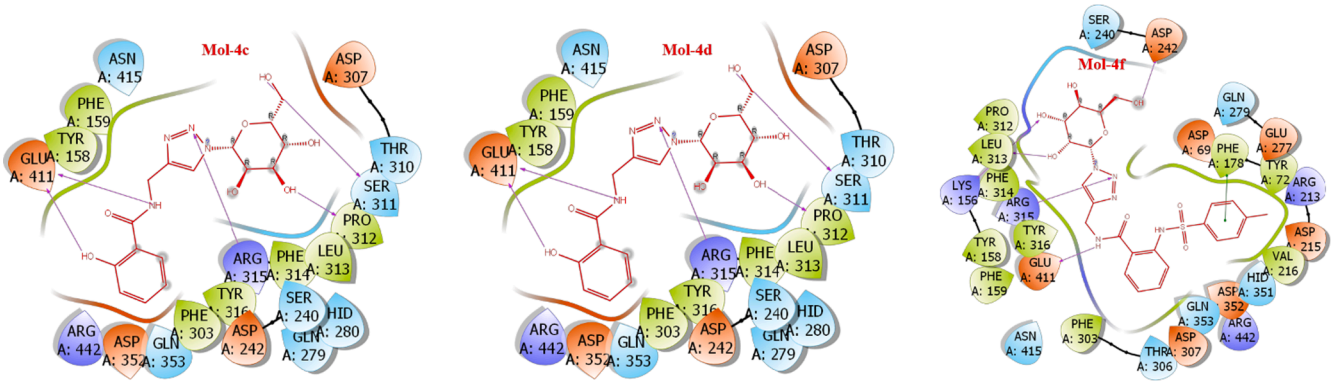

Fig 5. Figure showing different interactions in best docked posed protein–ligand complexes.

Table 4
Table representing various docking results.

S. No.	Molecule	3A4A Docking Score (kcal/mol)	Glide Score
1.	**Mol-4c**	−7.526	−7.555
2.	**Mol-4d**	−7.526	−7.555
3.	**Mol-4f**	−7.865	−7.893

in an octahedral box using the TIP3P water model at 298 K [56]. Counter ions were then added to the solvated box containing the protein–ligand complex by randomly replacing the water molecules to neutralize the system. Particle Mesh Ewald (PME) was used to handle long-range electrostatic interactions in periodic boundary conditions [57]. Energy minimization of the whole system was carried out in 25,000 steps using Steepest Descent leap- Frog Integration Method followed by NVT ensemble equilibration at a constant temperature of 300 K for the 50 s using Berendsen thermostat [58]. The system was then equilibrated with NPT ensemble at a constant pressure of 1 atm in 25,000 steps using steepest descent leap-frog integrator [59]. Particle Mesh Ewald (PME) was used to handle long-range electrostatic interactions in periodic boundary conditions and all the bonds involving hydrogen atoms were constrained using the LINCS algorithm [60]. Graphs were plotted using XMgrace software [61].

7. Results and discussion

This study was aimed to complement the experimental results and observations obtained, through means of computer simulations. It also included the identification of new leads, targeting the ligand-binding affinity, structural stability and applicability for the experimentally active ligands with protein. The results obtained through computer simulations are summarized and discussed as follows:

7.1. Molecular docking

The selected active ligands (Mol-4c, Mol-4d & Mol-4f) were docked to 3A4A protein in search of the interacting residues against the best docked posed complexes (Fig. 5). The docking results, corresponding to the selected protein sequences are summarized below in table 4. Various studies have been done to understand the docking studies of ligand-bound biological macromolecules [62]. Docking calculations revealed that all three biologically active molecules had comparable docking energies and Glide scores. And this result validates the fact that experimentally active molecules have good as well as comparable docking & Glide scores.

The key amino acid residues that are involved in the docking calculations are discussed in the forthcoming hydrogen bonding analysis section.

7.2. Hydrogen bonding analysis

Following Fig. 6 & Fig. 7 represent the binding site and corresponding H-donor/acceptor clouded regions near those hydrogen

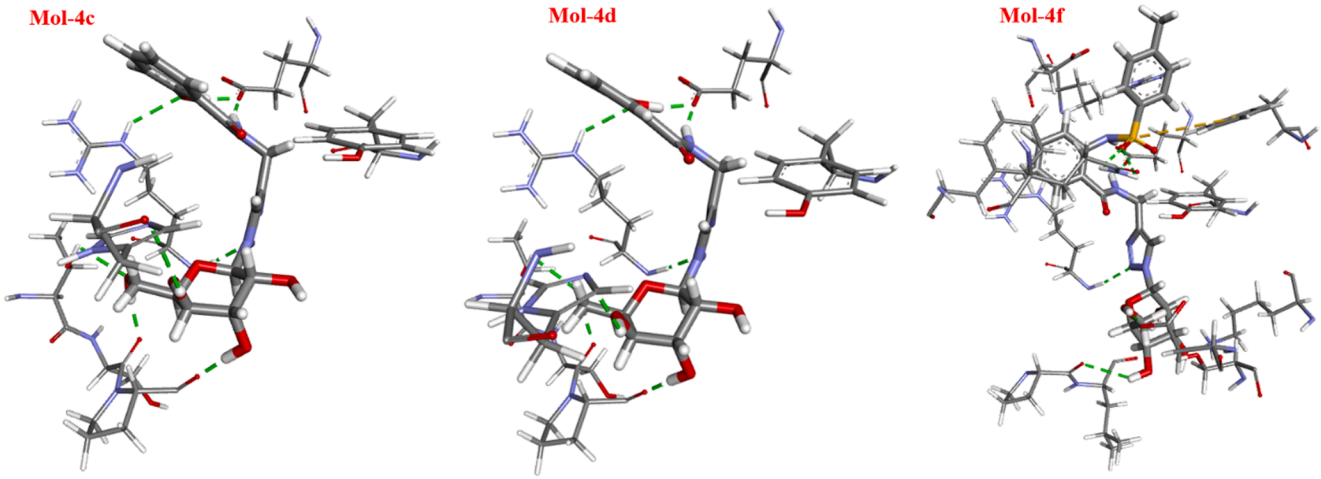

Fig 6. H-interaction sites for Mol-4c, Mol-4d & Mol-4f with 3A4A.

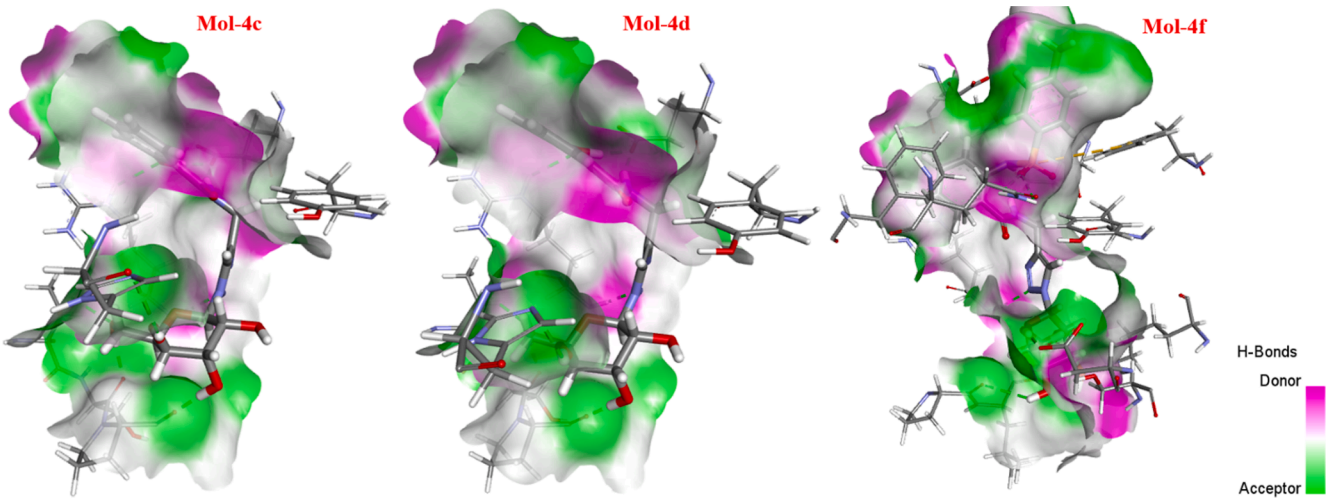

Fig 7. H-interaction cloud for Mol-4c, Mol-4d & Mol-4f with 3A4A.

Table 5
The following table represents the donor and the acceptor amino acid residues involved in the formation of a hydrogen bond between the PROTEIN and ligand atoms.

S. No.	Complex	No of H-bonds Formed	Interacting Species in H-Bonding	H-Bond Length (Å)
1	3A4A + Mol-4c	8	ARG315:HE - LIG900: O6 LIG900:H16 - GLU411: OE2 LIG900:H15 - GLU411: OE2 ARG315:H - LIG900:N2 LIG900:H9 - HIS280: NE2 THR310:HG1 - LIG900: O1 LIG900:H1 - SER311:O LIG900:*H*10 - PRO312: O	2.609662 1.638967 1.775453 2.119318 2.823075 2.716957 1.948873 1.629865
2	3A4A + Mol-4d	8	LIG900:H16 - GLU411: OE2 LIG900:H15 - GLU411: OE2 ARG315:HE - LIG900: O6 ARG315:H - LIG900:N2 THR310:HG1 - LIG900: O1 LIG900:H1 - SER311:O LIG900:H9 - HIS280: NE2 LIG900:*H*10 - PRO312: O	1.638967 1.775453 2.609662 2.119318 2.716957 1.948873 2.823075 1.629865
3	3A4A + Mol-4f	8	LYS156:HZ2 - LIG900: O4 LIG900:*H*11 - LEU313:O LIG900:H1 - ASP242: OD2 LIG900:H9 - A:PRO312: O ARG315:H - LIG900:N2 GLN279:HE21 - LIG900: O8 GLN279:HE22 - LIG900: O8 LIG900:H15 - GLU411: OE2	2.104894 1.967705 1.774475 2.820494 2.454007 2.839473 3.062884 2.161487

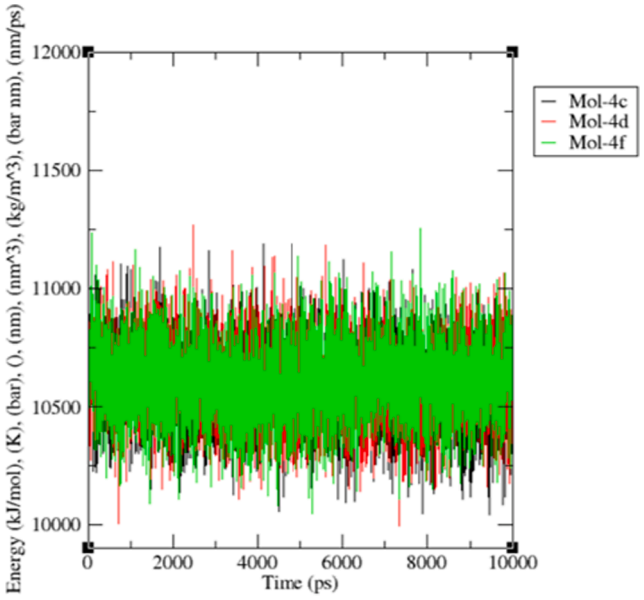

Fig 8. Figure depicting variation in energy of the system.

bonding sites, using Discovery Studio Visualizer [63]. This data gives us more detailed information about the docking results and the existence of H-bonds and key amino acid residues in the formation of H-bonds. Table 5 gives information about the donor and the acceptor amino acid residues involved in the formation of the hydrogen bond between the protein and ligand atoms, along with their respective bond lengths.

7.3. Molecular dynamics simulation

Structural stability of biomolecules under a specifically mimicked environment for a pre-defined period can be studied via molecular dynamics simulations. Such studies are of significant importance in the structure and dynamics of biomolecules owing to less experimental costs. Here in this study, various parameters were studied and analyzed for their biological validation and are discussed as follows:

7.3.1. Energy variations-

The energy variations obtained from molecular dynamics simulation of 3A4A for a time scale of 10000 ps are shown in Fig. 8. The variations in the energies of all the two ligand–protein complexes are comparable.

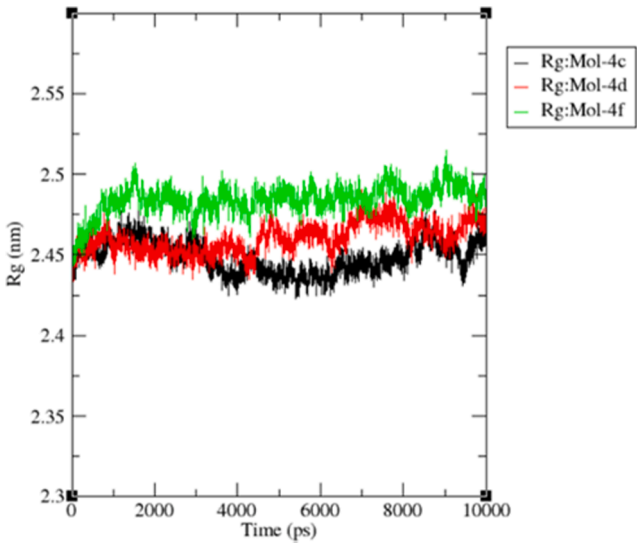

Fig 9. Fig representing variations for Radius of Gyration.

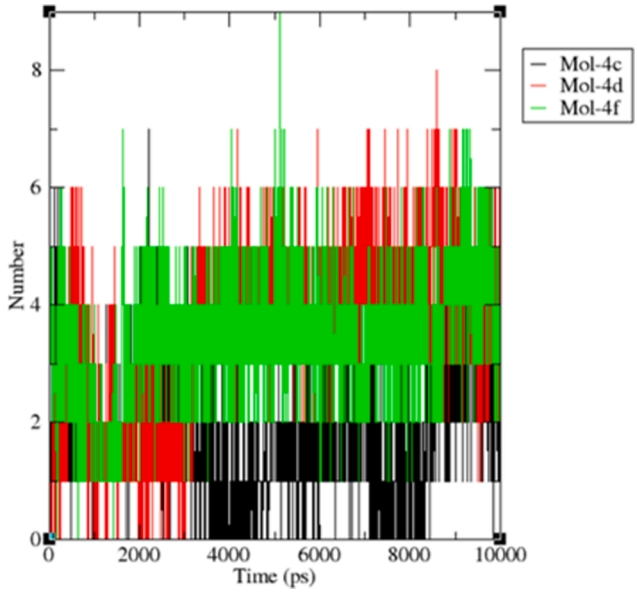

Fig 10. Variation in No. of H-bonds for protein–ligand complexes.

And hence the confirmation of stable complex formation requires analysis from various other perspectives viz., interactions and conformational stabilities, etc. of protein–ligand complexes.

7.3.2. Variation in radius of Gyration-

Radii of Gyration values are determined t understand the dynamic stability and compactness of protein–ligand complexes. The variation in radius of gyration of protein–ligand complexes can be seen from Fig. 9. The avg. radiuses of gyration for all the three protein–ligand complexes lie between 2.425 nm and 2.5 nm resp. These variation results reveal that protein sequence remains compact for the whole 10000 ps molecular dynamics simulation and hence confirms the stability of the complexes.

7.3.3. Variation in number of hydrogen bonds-

Hydrogen bonds play a crucial role in determining the binding affinity as well as binding specificity in protein–ligand interactions. Fig. 10 depicts the average number of hydrogen bonds being formed during the molecular dynamics trajectory for 10000 ps. Further, it can

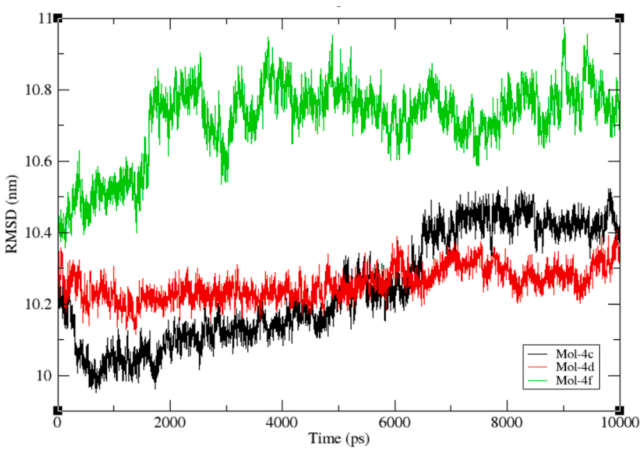

Fig 11. RMSD for protein–ligand complexes.

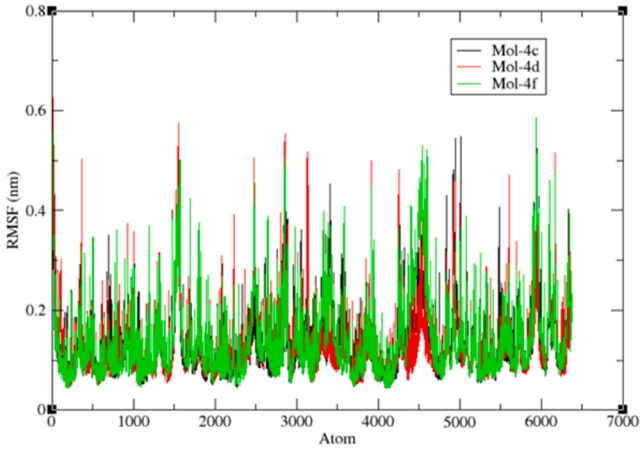

Fig 12. RMSF for protein–ligand complexes.

be seen from the figure that mol-4c could form an average of 7H-bonds, mol-4d could form an average of 8H-bonds whereas the maximum number of H-bonds formed by mol-4f is 9. This suggests the stronger interaction between all the three protein–ligand complexes and hence gets validated from the docking results also.

7.3.4. Root mean square deviation-

The RMSD is treated as the measure of conformational stability. The plots for RMSD of all the ligand- PROTEIN complexes are represented in Fig. 11. From the RMSD graph shown below, it can be seen that for Mol-4c & Mol-4d the RMSD range is between 10 ~ 10.4 Å whereas for Mol-4f the RMSD range lies between 10.4 ~ 10.8 Å; but the RMSD for Mol-4f shows stabilizing variations towards the end of the simulations and hence claim its stability than Mol-4c & Mol-4d.

7.3.5. Root mean square Fluctuation-

RMSF give us information about the fluctuation of each amino acid along with the fluctuations in the flexible regions of the protein during molecular dynamics simulation. The graphs shown below in Fig. 12 suggest that all the three protein–ligand complexes had comparable RMSF and therefore they contribute significantly towards the stability of the complexes. Here this range lies between 0.1 ~ 0.4 Å.

8. Conclusion

In conclusion, we have synthesized novel glycosyl methyl benzamide analogues with 1,4-regioselectivity employing the well-known CuAAC

reaction of the propylated benzamides with different sugar azides in the ambient condition in very good yields. These compounds were evaluated for α-glucosidase enzyme inhibitory activity and three compounds **4f**, **4d** and**4c** exhibited 42.9%, 40.6%, and 39.7%inhibition, respectively as compared to standard drug acarbose having 53.4% inhibition of the enzyme. Additionally, the docking results generated best docked posed complexes and proved to validate the findings of the experiments and complimented them very well. Further, when these docked complexes, when subjected to molecular dynamics, the results obtained also validated the findings of the docking & experimental results. Therefore, it can be concluded that computational techniques confirmed the stability of the active molecules and hence add to the validation of the experimental results. Thus, these glycosyl methyl benzamide analogues hold potential to be developed as antidiabetic agents.

Declaration of Competing Interest

The authors declare that they have no known competing financial interests or personal relationships that could have appeared to influence the work reported in this paper.

Acknowledgements

The authors AP and MKS are thankful to ICMR RA fellowship, Govt. of India, New Delhi and AKS is thankful to University-UGC fellowship for financial assistance and Dr Abhinay Pandey for providing biological data.

References

[1] R.W. Grant, N.G. Devita, D.E. Singer, J.B. Meigs, Polypharmacy and medication adherence in patients with type 2 diabetes, Diabetes Care 26 (2003) 1408–1412.
[2] C. Albuquerque, C. Correia, M. Ferreira, Adherence to the therapeutic regime in person with type 2 diabetes, Procedia-Social and Behavioral Sciences 171 (2015) 350–358.
[3] Z. Bonger, S. Shiferaw, E.Z. Tariku, Adherence to diabetic self-care practices and its associated factors among patients with type 2 diabetes in Addis Ababa, Ethiopia. Patient preference and adherence 12 (2018) 963.
[4] Meena SN, Naik MM, Ghadi SC, Tilve SG. α-Glucosidase inhibition activity and in silico study of 2-(benzo [d][1, 3] dioxol-5-yl)-4H-chromen-4-one, a synthetic derivative of flavone. Bioorganic & medicinal chemistry 2018.
[5] N. Cho, J. Shaw, S. Karuranga, Y. Huang, F.J. da Rocha, A. Ohlrogge, et al., IDF Diabetes Atlas: Global estimates of diabetes prevalence for 2017 and projections for 2045, Diabetes Res. Clin. Pract. 138 (2018) 271–281.
[6] P. Zimmet, K.G. Alberti, D.J. Magliano, P.H. Bennett, Diabetes mellitus statistics on prevalence and mortality: facts and fallacies, Nature Reviews Endocrinology 12 (2016) 616.
[7] V. Kren, L. Martínková, Glycosides in medicine:"The role of glycosidic residue in biological activity", Curr. Med. Chem. 8 (2001) 1303–1328.
[8] C.R. Bertozzi, L.L. Kiessling, Chemical glycobiology, Science 291 (2001) 2357–2364.
[9] C.D. Hein, X.-M. Liu, D. Wang, Click chemistry, a powerful tool for pharmaceutical sciences, Pharm. Res. 25 (2008) 2216–2230.
[10] K Tiwari V, C Mishra R, Sharma A, P Tripathi R. Carbohydrate based potential chemotherapeutic agents: recent developments and their scope in future drug discovery. Mini reviews in medicinal chemistry 2012;12:1497-519.
[11] V.K. Tiwari, B.B. Mishra, K.B. Mishra, N. Mishra, A.S. Singh, X. Chen, Cu-catalyzed click reaction in carbohydrate chemistry, Chem. Rev. 116 (2016) 3086–3240.
[12] G. Horne, F.X. Wilson, J. Tinsley, D.H. Williams, R. Storer, Iminosugars past, present and future: medicines for tomorrow, Drug Discovery Today 16 (2011) 107–118.
[13] T. Hara, J. Nakamura, N. Koh, F. Sakakibara, N. Takeuchi, N. Hotta, An importance of carbohydrate ingestion for the expression of the effect of α-glucosidase inhibitor in NIDDM, Diabetes Care 19 (1996) 642–647.
[14] M. Toeller, α-Glucosidase inhibitors in diabetes: efficacy in NIDDM subjects, Eur. J. Clin. Invest. 24 (1994) 31–35.
[15] A.E. Martin, P.A. Montgomery, Acarbose: an alpha-glucosidase inhibitor, American Journal of Health-System Pharmacy 53 (1996) 2277–2290.
[16] L. Amini-Rentsch, E. Vanoli, S. Richard-Bildstein, R. Marti, G. Vilé, A Novel and Efficient Continuous-Flow Route To Prepare Trifluoromethylated N-Fused Heterocycles for Drug Discovery and Pharmaceutical Manufacturing, Ind. Eng. Chem. Res. 58 (2019) 10164–10171.
[17] L. Jiang, M.-Y. Wang, F.-X. Wan, Z.-Q. Qu, Synthesis and biological activity of tri-substituted 1, 2, 4-triazoles bearing benzimidazole moiety, Phosphorus, Sulfur, and Silicon and the Related Elements 190 (2015) 1599–1605.
[18] T. Ertan, I. Yildiz, S. Ozkan, O. Temiz-Arpaci, F. Kaynak, I. Yalcin, et al., Synthesis and biological evaluation of new N-(2-hydroxy-4 (or 5)-nitro/aminophenyl) benzamides and phenylacetamides as antimicrobial agents, Bioorg. Med. Chem. 15 (2007) 2032–2044.
[19] A. Pau, G. Boatto, M. Palomba, B. Asproni, R. Cerri, F. Palagiano, et al., Synthesis of N-[4-(alkyl) cyclohexyl]-substituted benzamides with anti-inflammatory and analgesic activities, Il Farmaco 54 (1999) 524–532.
[20] R. Tandon, I. Singh, V. Luxami, N. Tandon, K. Paul, Recent Advances and Developments of in vitro Evaluation of Heterocyclic Moieties on Cancer Cell Lines, The Chemical Record 19 (2019) 362–393.
[21] K. Amin, M. Kamel, M. Anwar, M. Khedr, Y. Syam, Synthesis, biological evaluation and molecular docking of novel series of spiro [(2H, 3H) quinazoline-2, 1′-cyclohexan]-4 (1H)-one derivatives as anti-inflammatory and analgesic agents, Eur. J. Med. Chem. 45 (2010) 2117–2131.
[22] A.D. Cale Jr, T.W. Gero, K.R. Walker, Y.S. Lo, W.J. Welstead Jr, L.W. Jaques, et al., Benzo-and pyrido-1, 4-oxazepin-5-ones and-thiones: Synthesis and structure-activity relationships of a new series of H1-antihistamines, J. Med. Chem. 32 (1989) 2178–2199.
[23] I. Irwin, M. Palme, C. Becker, P. Druzgala, Stereoisomeric compounds and methods for the treatment of gastrointestinal and central nervous system disorders, Google Patents (2012).
[24] N. Charaya, D. Pandita, A.S. Grewal, V. Lather, Design, synthesis and biological evaluation of novel thiazol-2-yl benzamide derivatives as glucokinase activators, Comput. Biol. Chem. 73 (2018) 221–229.
[25] X.-L. Wang, K. Wan, C.-H. Zhou, Synthesis of novel sulfanilamide-derived 1, 2, 3-triazoles and their evaluation for antibacterial and antifungal activities, Eur. J. Med. Chem. 45 (2010) 4631–4639.
[26] A. Singh, C. Biot, A. Viljoen, C. Dupont, L. Kremer, K. Kumar, et al., 1H–1, 2, 3-triazole-tethered uracil-ferrocene and uracil-ferrocenylchalcone conjugates: Synthesis and antitubercular evaluation, Chem. Biol. Drug Des. 89 (2017) 856–861.
[27] S. Zhang, Z. Xu, C. Gao, Q.-C. Ren, L. Chang, Z.-S. Lv, et al., Triazole derivatives and their anti-tubercular activity, Eur. J. Med. Chem. 138 (2017) 501–513.
[28] N. Ma, Y. Wang, B.-X. Zhao, W.-C. Ye, S. Jiang, The application of click chemistry in the synthesis of agents with anticancer activity, Drug design, development and therapy 9 (2015) 1585.
[29] I. Mohammed, I.R. Kummetha, G. Singh, N. Sharova, G. Lichinchi, J. Dang, et al., 1, 2, 3-triazoles as amide bioisosteres: discovery of a new class of potent HIV-1 Vif antagonists, J. Med. Chem. 59 (2016) 7677–7682.
[30] M. Whiting, J. Muldoon, Y.C. Lin, S.M. Silverman, W. Lindstrom, A.J. Olson, et al., Inhibitors of HIV-1 protease by using in situ click chemistry, Angew. Chem. Int. Ed. 45 (2006) 1435–1439.
[31] da Silva FdC, do Carmo Cardoso MF, Ferreira PG, Ferreira VF. Biological Properties of 1H-1, 2, 3-and 2H-1, 2, 3-Triazoles. Chemistry of 1, 2, 3-triazoles: Springer; 2014. p. 117-65.
[32] W.G. Lewis, L.G. Green, F. Grynszpan, Z. Radić, P.R. Carlier, P. Taylor, et al., Click chemistry in situ: acetylcholinesterase as a reaction vessel for the selective assembly of a femtomolar inhibitor from an array of building blocks, Angew. Chem. Int. Ed. 41 (2002) 1053–1057.
[33] N.R. Emmadi, C. Bingi, S.S. Kotapalli, R. Ummanni, J.B. Nanubolu, K. Atmakur, Synthesis and evaluation of novel fluorinated pyrazolo-1, 2, 3-triazole hybrids as antimycobacterial agents, Bioorg. Med. Chem. Lett. 25 (2015) 2918–2922.
[34] R. Périon, V. Ferrières, M.I. Garcia-Moreno, C.O. Mellet, R. Duval, J.M. G. Fernández, et al., 1, 2, 3-Triazoles and related glycoconjugates as new glycosidase inhibitors, Tetrahedron 61 (2005) 9118–9128.
[35] K. Slámová, P. Marhol, K. Bezouška, L. Lindkvist, S.G. Hansen, V. Křen, et al., Synthesis and biological activity of glycosyl-1H-1, 2, 3-triazoles, Bioorg. Med. Chem. Lett. 20 (2010) 4263–4265.
[36] G. Wang, Z. Peng, J. Wang, J. Li, X. Li, Synthesis and biological evaluation of novel 2, 4, 5-triarylimidazole–1, 2, 3-triazole derivatives via click chemistry as α-glucosidase inhibitors, Bioorg. Med. Chem. Lett. 26 (2016) 5719–5723.
[37] A. Sharma, S. Sharma, R.P. Tripathi, R.S. Ampapathi, Robust turn structures in α3β cyclic tetrapeptides induced and controlled by carbo-β3 amino acid, The Journal of organic chemistry 77 (2012) 2001–2007.
[38] H. Twin, R.A. Batey, Intramolecular hetero Diels– Alder (Povarov) approach to the synthesis of the alkaloids luotonin a and camptothecin, Org. Lett. 6 (2004) 4913–4916.
[39] M.-G. Braun, M.H. Katcher, A.G. Doyle, Carbofluorination via a palladium-catalyzed cascade reaction, Chem. Sci. 4 (2013) 1216–1220.
[40] M. Goebel, H.-G. Nothofer, G. Roß, I. Ugi, A facile synthesis of per-O-alkylated glycono-δ-lactones from per-O-alkylated glycopyranosides and a novel ring contraction for pyranoses, Tetrahedron 53 (1997) 3123–3134.
[41] M. Masuda, T. Shimizu, Synthesis of Novel α, ω-Type 1-Glucosamide and 1-Galactosamide Bolaamphiphiles, J. Carbohydr. Chem. 17 (1998) 405–416.
[42] R.K. Thakur, A. Mishra, K. Ramakrishna, R. Mahar, S.K. Shukla, A. Srivastava, et al., Synthesis of novel pyrimidine nucleoside analogues owning multiple bases/sugars and their glycosidase inhibitory activity, Tetrahedron 70 (2014) 8462–8473.
[43] A. Khan, V. Tiwari, R. Ahmad, A. Srivastava, R. Tripathi, Synthesis of α-Mannosylated Phenolics as α-Glucosidase Inhibitors, J. Enzyme Inhib. Med. Chem. 19 (2004) 107–112.
[44] G. Hübscher, G. West, Specific assays of some phosphatases in subcellular fractions of small intestinal mucosa, Nature 205 (1965) 799–800.
[45] K. Yamamoto, H. Miyake, M. Kusunoki, S. Osaki, Crystal structures of isomaltase from Saccharomyces cerevisiae and in complex with its competitive inhibitor maltose, The FEBS journal 277 (2010) 4205–4214.
[46] H.M. Berman, T. Battistuz, T.N. Bhat, W.F. Bluhm, P.E. Bourne, K. Burkhardt, et al., The protein data bank, Acta Crystallogr. D Biol. Crystallogr. 58 (2002) 899–907.

[47] E.F. Pettersen, T.D. Goddard, C.C. Huang, G.S. Couch, D.M. Greenblatt, E.C. Meng, et al., UCSF Chimera—a visualization system for exploratory research and analysis, J. Comput. Chem. 25 (2004) 1605–1612.
[48] R. Yadav, A. Pandey, N. Awasthi, A. Shukla, Molecular Docking Studies of Enzyme Binding Drugs on Family of Cytochrome P450, Advanced Science, Engineering and Medicine 12 (2020) 83–87.
[49] Shukla A, Mishra R, Pandey A, Dwivedi A, Kumar D. Interaction of Flavonols with DNA: Molecular Docking Studies. PROCEEDING OF INTERNATIONAL SYMPOSIUM ON ADVANCES IN FUNCTIONAL AND BIOLOGICAL MATERIALS (ISAFBM-2019)2019. p. 4.
[50] R. Mishra, A. Kumar, R. Chandra, D. Kumar, A review on theoretical studies of various types of Drug-DNA Interaction, International Journal of Science, Technology and Society 3 (2017) 11–27.
[51] E. Kellenberger, J. Rodrigo, P. Muller, D. Rognan, Comparative evaluation of eight docking tools for docking and virtual screening accuracy, Proteins Struct. Funct. Bioinf. 57 (2004) 225–242.
[52] H. Zhao, A. Caflisch, Molecular dynamics in drug design, Eur. J. Med. Chem. 91 (2015) 4–14.
[53] M. Abraham, T. Murtola, R. Schulz, S. Páll, J. Smith, B. Hess, et al., Gromacs: High performance molecular simulations through multi-level parallelism from laptops to supercomputers, SoftwareX 1 (2015) 19–25.
[54] W. Huang, Z. Lin, W.F. van Gunsteren, Validation of the GROMOS 54A7 force field with respect to β-peptide folding, J. Chem. Theory Comput. 7 (2011) 1237–1243.
[55] A.W. Schüttelkopf, D.M. Van Aalten, PRODRG: a tool for high-throughput crystallography of protein–ligand complexes, Acta Crystallogr. D Biol. Crystallogr. 60 (2004) 1355–1363.
[56] P. Mark, L. Nilsson, Structure and dynamics of the TIP3P, SPC, and SPC/E water models at 298 K, Journal of Physical Chemistry A 105 (2001) 9954–9960.
[57] T. Darden, D. York, L. Pedersen, Particle mesh Ewald: an N* log (N) method for computing Ewald sums, J. Chem. Phys. 98 (1993) 10089–10092.
[58] J.-P. Ryckaert, G. Ciccotti, H.J. Berendsen, Numerical integration of the cartesian equations of motion of a system with constraints: molecular dynamics of n-alkanes, J. Comput. Phys. 23 (1977) 327–341.
[59] B. Hess, H. Bekker, H.J. Berendsen, J.G. Fraaije, LINCS: a linear constraint solver for molecular simulations, J. Comput. Chem. 18 (1997) 1463–1472.
[60] Turner P. XMGRACE, Version 5.1. 19. Center for Coastal and Land-Margin Research, Oregon Graduate Institute of Science and Technology, Beaverton, OR 2005.
[61] A. Pandey, R. Mishra, A. Yadav, Understanding interactions of DNA minor groove binders using advanced computational techniques, Int J Anal Exp Modal Anal 12 (2020) 1300–1315.
[62] Pandey A, Mishra R, Shukla A, Yadav AK, Kumar D. In-silico docking studies of 2, 5-bis (4-amidinophenyl) furan and its derivatives. PROCEEDING OF INTERNATIONAL SYMPOSIUM ON ADVANCES IN FUNCTIONAL AND BIOLOGICAL MATERIALS (ISAFBM-2019)2019. p. 11.
[63] D.S. Biovia, Discovery studio modeling environment, Release (2017).